SAE Aero Design East 2020

DJS
SKYLARK

Team Name: DJS SKYLARK – MICRO CLASS

Team Number: 312

School Name: Dwarkadas J Sanghvi College of Engineering

TEAM MEMBERS
Team Captain: Fenil Vanani

Harmin Naik	Sucheta Kabra
Glenn Castellino	Rishi Dasgupta
Chaitrali Chaudhari	Jainam Gala
Muskaan Mehta	Aayush Shah
Rushabh Gala	Siddharth Singh
Ved Vartak	Rishi Ghia
Dhairya Foria	Raj Anadkat
Sharva Potdar	Roshan Sam
Shome Vakharia	Hiral Shah
Nainika Shah	Riyanshi Shah
Kirtan Jhaveri	Nishita Mehta
Durvesh Deokar	Shantanu Thorat
Gaurang Raje	Jinay Gandhi
Heta Shah	

STATEMENT OF COMPLIANCE

Certification of Qualification

Team Name	DJS Skylark – Micro Class	Team Number	312

School   Dwarkadas J. Sanghvi College of Engineering

Faculty Advisor   Prof. Shashikant Auti

Faculty Advisor's Email   shashikant.auti@gmail.com
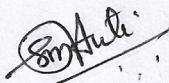
Statement of Compliance

As faculty Adviser:

_SA_ (Initial) I certify that the registered team members are enrolled in collegiate courses.
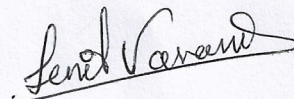
_SA_ (Initial) I certify that this team has designed and constructed the radio controlled aircraft in the past nine (9) months with the intention to use this radio controlled aircraft in the 2020 SAE Aero Design competition, without direct assistance from professional engineers, R/C model experts, and/or related professionals.

_SA_ (Initial) I certify that this year's Design Report has original content written by members of this year's team.

_SA_ (Initial) I certify that all reused content has been properly referenced and is in compliance with the University's plagiarism and reuse policies.

_____   _____
Signature of Faculty Advisor   Signature of Team Captain

Table of Contents

List of Symbols:

Symbol	Description	Symbol	Description
c	Chord of the control surface	S	Wing Planform Area
C_d	Drag coefficient of airfoil	S1	Maximum control surface deflection
C_l	Lift coefficient of airfoil	S2	Maximum servomotor deflection
C_D	Drag coefficient of aircraft	t	Time period
C_{Di}	Lift-induced drag coefficient	T	Thrust
C_{D0}	Zero-lift drag coefficient	v	Airspeed
C_L	Lift coefficient of aircraft	v*	Aircraft Corner Speed
C_M	Coefficient of pitching moment of aircraft	v_{gE}	Gust Equivalent Speed
d	Diameter of the propeller	v_d	Dive speed
D	Drag	v_e	Exit Velocity
g	Acceleration due to Gravity	W	Weight of the aircraft
I	Moment of Inertia	α	Angle of attack
L	Lift	β	Factor of correction in Thrust calculations
m	Mass of the aircraft	ρ	Density
n	Load factor	ω	Frequency
P	Payload mass	ζ	Damping Factor

List of Abbreviations:

Abbr.	Description	Abbr.	Description
CG	Centre of Gravity	MOS	Margin of Safety
FOS	Factor of Safety	TMA	Tail Moment Arm
MAC	Mean Aerodynamic Chord	UTM	Universal Testing Machine
CF	Carbon Fibre	PETG	Poly Ethylene Terephthalate - Glycol
3D	3-Dimensional	PLA	Polylactic Acid

List of Figures and Tables:

1.0   Executive Summary

1.1 System Overview and Discriminators

Integrated Avionics Bay

Avionics bay integrated into tail boom to reduce empty plane weight and assembly time.

Retractable Tail

Telescopic booms used to extend and retract tails for box fitting.

Dual Axis Stabilizer

Used to provide motion in two axes for combined elevator and rudder motion.
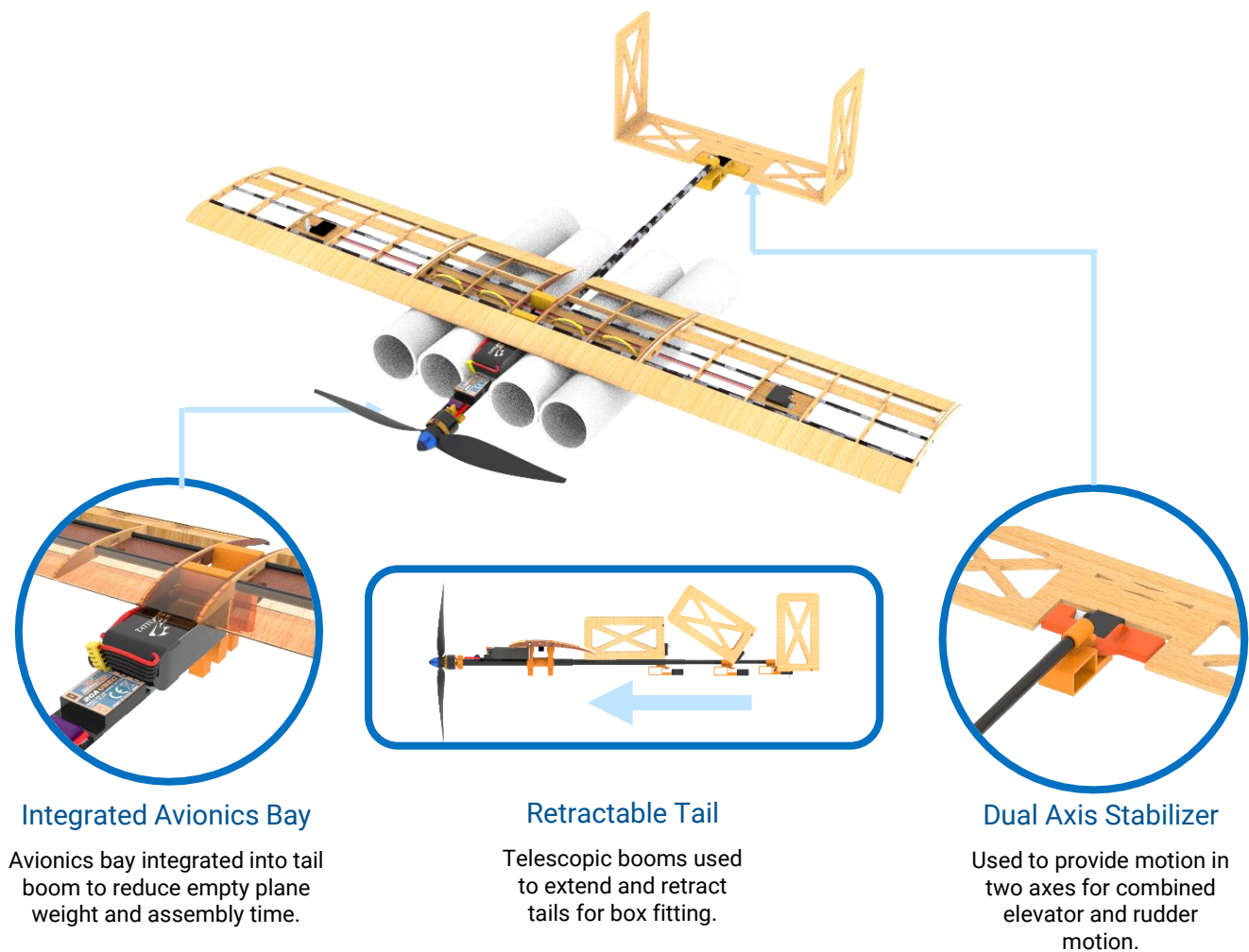
Figure 1(a): System Overview

Electronics		
Motor	**Propeller**	**Battery**
Sunnysky X2814-6 1250kV	13X4E	Tattu LiPo 1050mAh 3S 75C
Wings		
Airfoil	**Span**	**Planform**
Eppler E61	34.2"	Rectangular
Empannage		
Horizontal Tail	**Vertical Tail**	**Configuration**
Flat Plate Stabilator	Twin Flat Plate	U Tail

Table 1(b): Subsystem Details

1.2   Competition Projections

We aim to successfully fly with a payload fraction of 2.43 and complete our assembly demonstration within 15 seconds. This should result in a total flight score of 75.4 points, which combined with strong Design Report and Technical Presentation scores, will likely place us in the top 3 ranks. We have performed extensive testing and optimizations on the design and are confident of its performance at the competition.

2.0   Project Management

2.1   Schedule Summary

We started working in July, optimizing our previous year's design by exploring alternatives to various design choices. Our schedule was structured into monthly cycles of design, testing and optimization, working around our exam schedule and conducting an annual aeromodelling workshop.
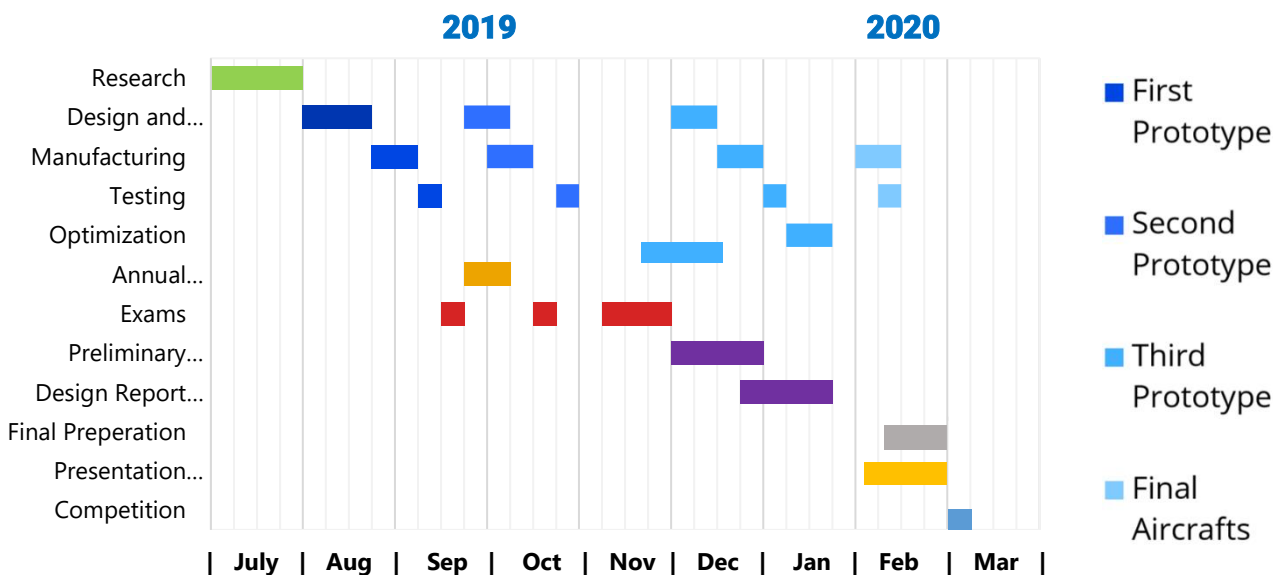

Figure 2(a): Schedule Summary

2.2   Personnel Management

Comprising of 28 students, the team was segregated into aerodynamics, structural, avionics and marketing departments. Each department had specific individuals assigned to a class while continuing to work as a single group. This ensured that ideas could be shared and discussed effectively within and in between departments, allowing simultaneous progress in both the classes. Over time, Design Report and Technical Presentation groups were also formed.

2.3   Cost Report
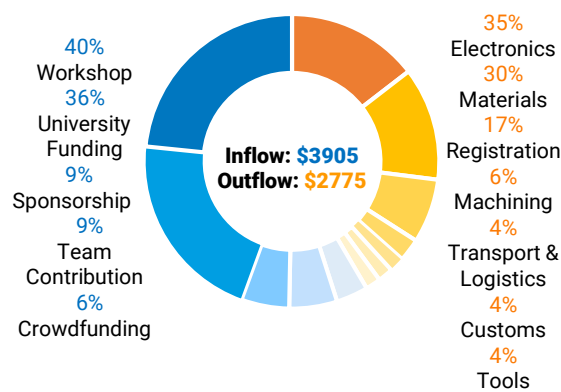
Figure 2(b): Cost Summary
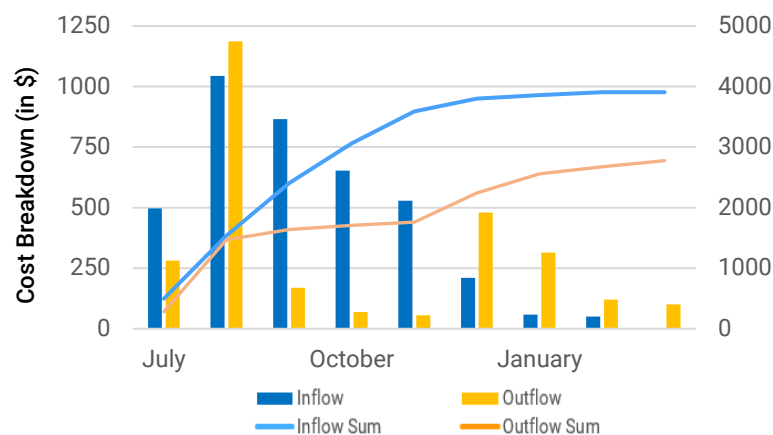
Figure 2(c): Schedule and Cost Breakdown

The outflow of funds largely comprised of electronic components, raw material procurement, manufacturing tools, registration fee and logistics. Starting off with university funding received in August, we raised funds through sponsorships and crowdfunding throughout the year. In September we organized an annual aero-modelling workshop for aero enthusiasts across Mumbai to raise additional funds, ensuring sustainability. To reduce the high costs of material procurement, we contacted international wholesalers directly. Heavy customs duty and long shipping periods limited our options for testing electronics. However, we overcame this by using online tools to shortlist electronics before testing. **Figure 2(c)** represents how funds were managed through the year to eliminate any financial blockages in the Design Process and Manufacturing.

3.0   Design Layout and Trades

3.1 Design Layout

1. Wings

Airfoil
Eppler E61 (5.6% thickness) with 6.5" chord used in rectangular planform.

Aileron
Covers 24% of wing area

Payload Carriers
Rectangular plywood plates used along with zipties to attach pipes under the wing.
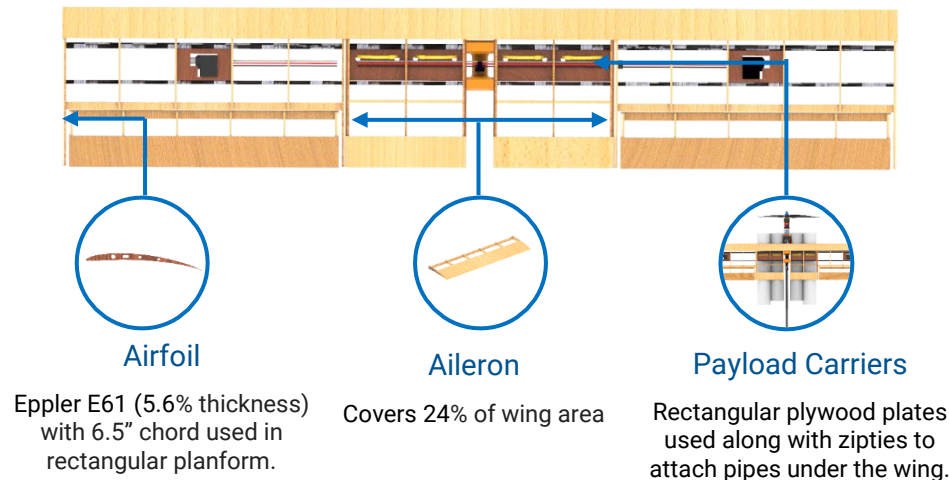
Figure 3(a): Wing Layout

The wing uses the Eppler E61 airfoil and has a span of 34.2" with 6.5" chord. It is made in three parts to be able to fit in the box. A hollow CF cylinder is used as the primary spar which slides into other co-axial CF tubes to integrate the wing into one part. We used magnets to maintain alignment for the sliding system and serve as secondary attachments. JR connectors placed at wing junctions are used as electrical and mechanical attachments.

2. Payload

The aircraft is designed to carry a total payload weight of 2.83lbs. It is divided into four pipes, with two each of 13" and 12" lengths. Pipes are attached to the wing with zip-ties which pass through slots on the pipe and through a basswood plate fixed in the wing.

3. Empennage

We designed a U-tail configuration keeping a TMA of 18.3". A dual axis rotor system was developed, with motion about each axis controlled independently by servos. This reduced the need for one more servo, reducing around 4% empty weight. A stabilizer configuration provides

higher pitching and yawing rates besides allowing efficient box fitting as it can be folded by 90º which reduces volume occupancy by 80%.

4. Fuselage

The fuselage comprises of three co-axial CF pipes, which slide into each other like a telescope occupying 65% less volume in the box. It is connected to the motor, wings and tails using 3-D printed connectors.

Horizontal Stabilizer
Covers 77% of tail area, hinged to rotate by 90º in retracted configuration.

Tail Moment Arm (TMA): 18.3"

Vertical Stabilizer
Rotation about perpendicular axis to generate yawing motion

Figure 3(b): Central Assembly

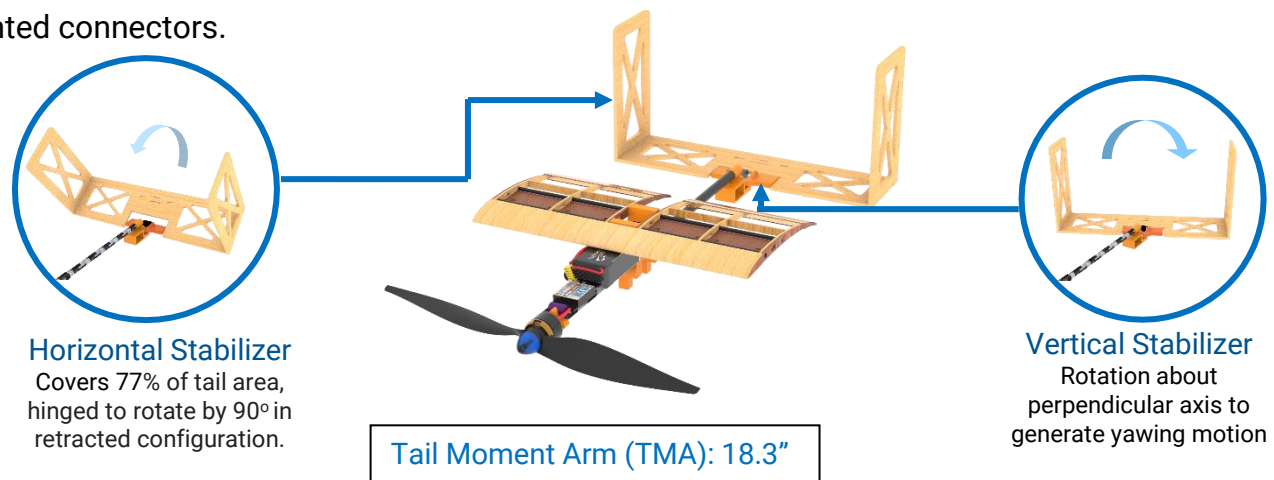## 5. 3-D Printed Connectors

We used 3-D printed parts made from PET-G which allowed us to create complex multi-purpose structural units while giving more control over component weights as parameters like wall count and infill percentage could be adjusted according to the required safety margins.

Motor Mount

Wing-Boom Connector

Dual Axis Connector
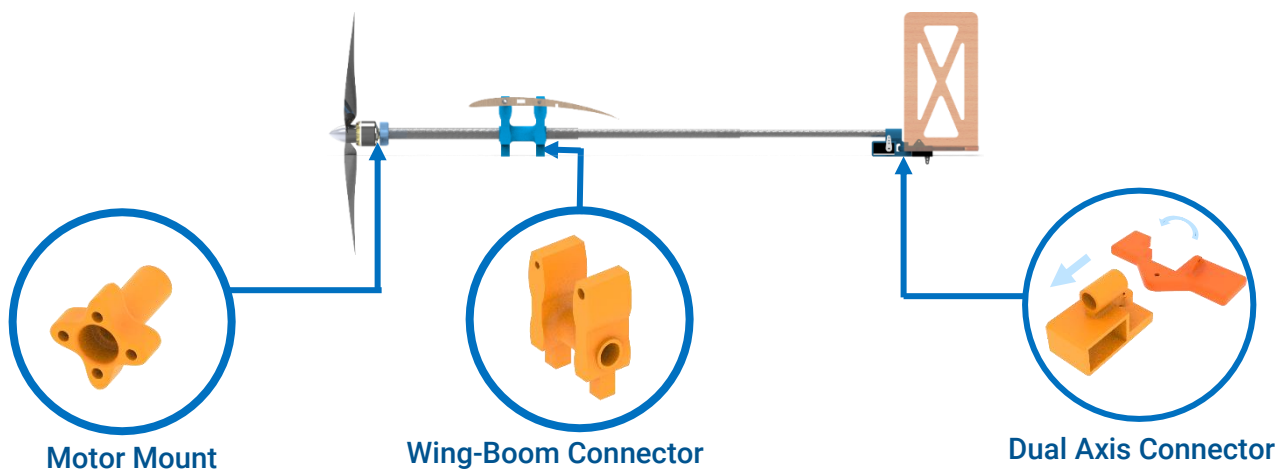
Figure 3(c): Connectors and Mountings

6. Electronics

Battery
Tattu 3S 1050mAh

ESC
Racerstar RS80A

Motor
SunnySky X2814-6
1250kV

Propeller
APC 13x4E

BEC
UBEC 3A, 5V

Aileron   – Turnigy 9018-MG
Elevator – Turnigy 9018-MG
Rudder   – Turnigy 9018-MG

Transmitter
FrSky Taranis X9D

Receiver
FrSky S6R with 3-axis stabilization

Servo
For actuating
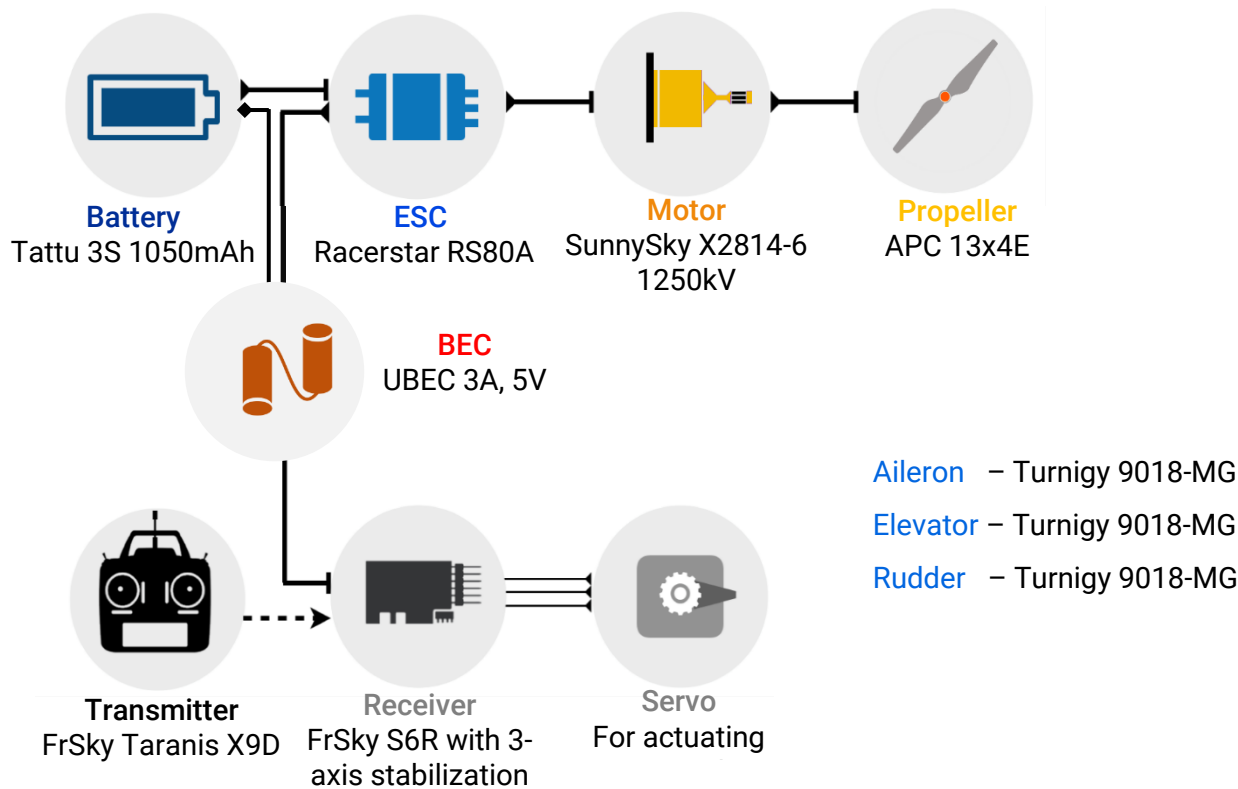
Figure 3(d): Electronics System Details

7. Container Specification

The aircraft system container is made from a single corrugated sheet of cardboard with a forward opening flap. This allows direct access to all components which reduces assembly time. The aircraft is stored as a central assembly which consists of fuselage attached to motor mount, tails and center wing, and 2 outer wings placed over the pipes. Telescopic tail boom is retracted and propeller is detached to allow more volume for pipe fitting. Two 3-D printed stands are kept in the box to hold the fuselage at a height in order to fit the pipes under it.

Figure 3(e): Container Assembly

3.2   Competitive Scoring and Strategy Analysis

Figure 3(f): Scoring Analysis
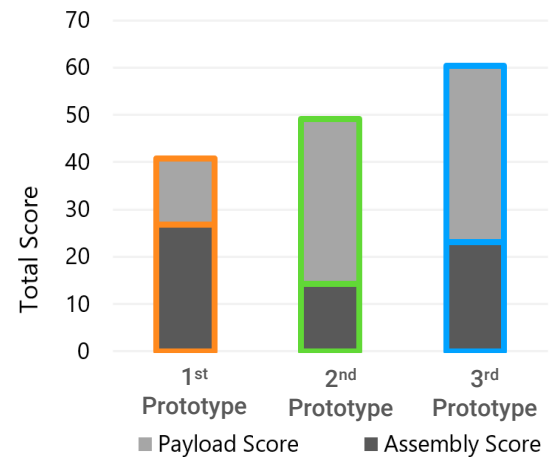
Figure 3(g): Prototypes Developed

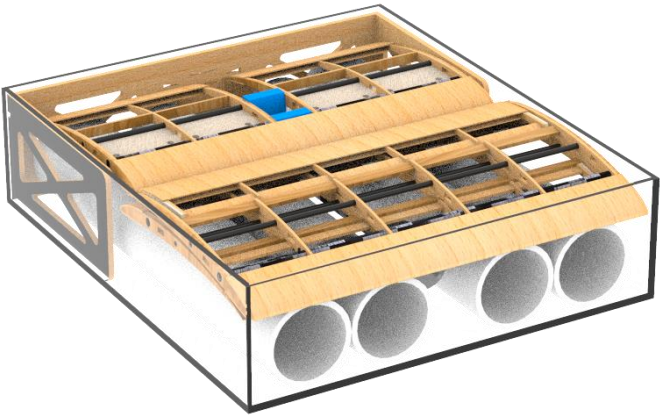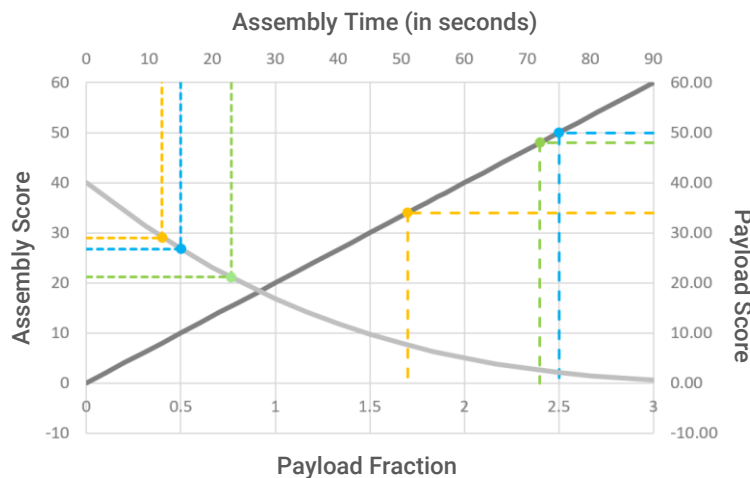We designed three prototypes through the year, prioritizing assembly time or payload fraction. A benchmark was set at 75 points, which could be achieved practically either by having a payload fraction of 2.2 with 10 seconds assembly time or payload fraction of 2.5 with assembly time of 17 seconds.

Our first aircraft was an EPS (Extruded Polystyrene) based flat plate flying wing design, which had minimum modular components for faster assembly. This design failed to meet our scoring criteria as the need for additional reinforcements increased empty aircraft weight and resulted in a payload fraction of 1.4, which would receive a total score of 55 points.

The second prototype was based on a conventional aircraft design which gave precedence to payload fraction over assembly time. We designed a five-part wing with 47" span and 5.8" chord, which provided significantly higher carrying capacity. As maximum payload is constrained by the box dimensions, this configuration had a payload fraction of 2.4, and with an assembly time of 23 seconds giving a total of 69 points.

The third prototype was designed to improve on the limitations of the previous designs. We rearranged components in the box and improved the ergonomics of attachment mechanisms.

The wing was designed to be in three-parts, with a span of 34.2" and 6.5" chord, capable of lifting the same payload. We achieved a payload fraction of 2.48 and assembly time of 15 seconds, giving a total score of 76.5 points.

We compromised on our empty weight to improve our propulsion system performance for the final design. This extended the design's performance limit, ensuring reliability through competition rounds.

3.3 Design Derivations

1. Wings
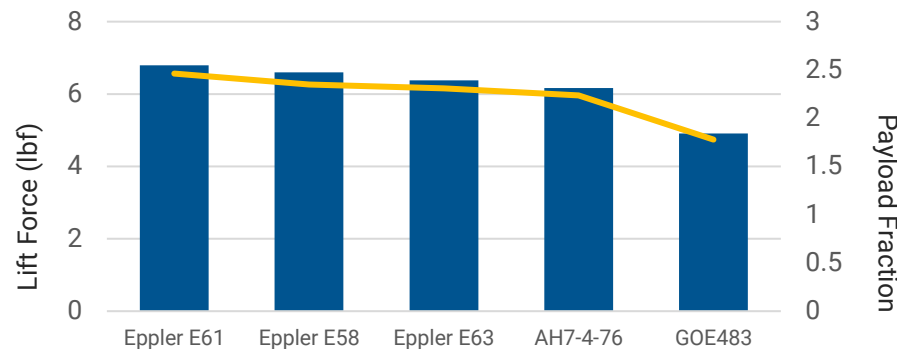
Figure 3(h): Planform Comparison

The wing was designed so as to fit maximum area in the box by placing it over the pipes. After the flying wing design with flat plate airfoil failed to reach the desired score, we started curating a list of airfoils based on geometry and C_L values. We found that a maximum of 7% airfoil thickness was compatible with the 3-part wing for box fitting. Among the shortlisted airfoils, Eppler E61 wing was found to be giving the maximum lift.

As the induced drag factor is minimal for this scale and operating velocity, rectangular planforms were considered to maximize area. To minimize assembly time, hollow wing extensions made from CF and PLA individually were designed and manufactured in the form of sliding channels for wing sections. However, this was rejected as the increase in empty weight compensated for the decrease in assembly time.

Initially, we developed a 5-part wing with 47" wingspan and 5.8" chord. We chose Eppler E61

(max thickness 5.7%) as it was giving the highest lifting capabilities. The chord was selected such that it allowed wing sections to be placed adjacent to each other and provide higher packing efficiency in the box. The design could carry greater amount of payload but the achievable payload fraction was restricted due to limitations of pipe fitting. This design was eventually rejected for higher assembly time and greater tip stalling tendencies which were evident from flight tests.

We developed on our second prototype by decreasing number of wing parts to 34.2" with 6.5" chord. Although wing area reduced by 18%, it could carry the same payload as greater velocities were achievable on the design to generate lift. The lower aspect ratio reduced the aircraft's tendency to tip stall as was observed in previous flight tests with the second prototype.

2. Fuselage/Tail Boom

A 3D printed connection is used to attach the central wing section to a CF boom. The fuselage is essentially a system of telescopic booms which can be retracted for maximum packing efficiency in the box. The motor is mounted directly onto the boom via a 3D printed firewall and the avionics bay is integrated with the boom itself. The wing is mounted 1.4" above the fuselage such that the pipe extends 1.3" beyond its base allowing it to take maximum impact loading at landing.

3. Payload:

A variety of 3-D printed fixtures based on cufflinks, plugs, sliders, hooks, clamps and other mechanisms were designed and tested. They were rejected as they failed to sustain flight loads for the required weights as they increased empty aircraft weight and required greater assembly time. We used zip-ties to attach the pipes as they proved to be the more durable and efficient.

4. Empennage
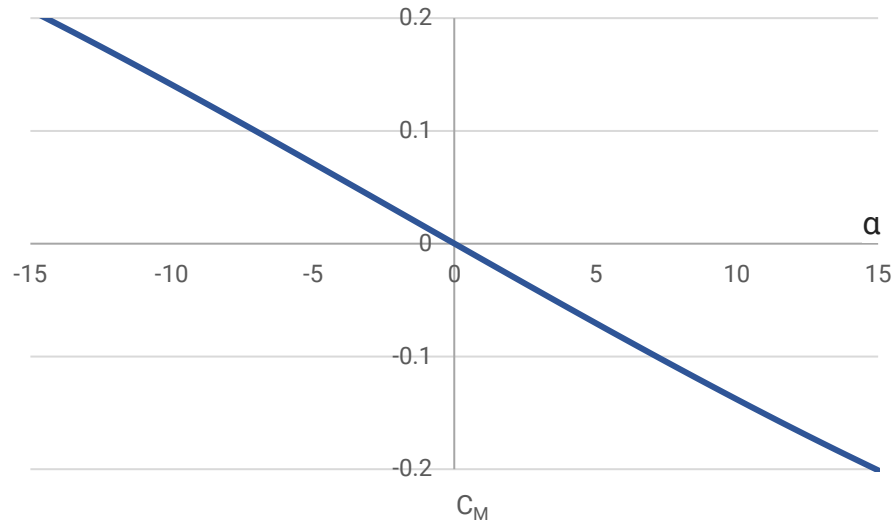
Figure 3(i): C_M Vs α

The empennage configuration was driven by container constraints and assembly time, as with all components. Inverted T and U configurations were considered for the tail design. The latter configuration fit well around the box constraints which was the primary objective. It also allowed to obtain the required tail volume coefficient at a lower TMA. Reducing TMA helped us save weight in tail boom and electrical connections length. Vertical tail is placed outside the prop wash region, delivering unhindered performance. We traded between airfoil shape and flat plate. The former gave better aerodynamic performance while the latter had better volume occupancy. We selected the latter as the aerodynamic performance loss was compensated by increasing area and was easy to manufacture.

5. Electronics

The selection of motor and propeller was based on dynamic performance analysis for various flight conditions like take-off, turning and cruising while comparing its weight. The required torque at the control surface hinge was calculated using the formula mentioned in Appendix A, at the dive speed of the aircraft. The torque available due to the servo at the hinge was found out as the servo arm and control horn lengths were known.

Control Surface	Servomotor	Rated Torque (oz-in)	Control Surface Deflection	Required Torque (oz-in)
Aileron	Turnigy 9018-MG	34.718	30°	4.0
Elevator	Turnigy 9018-MG	34.718	30°	9.5
Rudder	Turnigy 9018-MG	34.718	30°	5.1

Table 3(j): Electronics Specifications

6. Material allocation

Material selection was based on geometrical constraints and functionality of each component. Wing spars and tail boom were made with CF tubes, which incorporated a slider mechanism for wing attachment and telescopic extension of boom, while providing sufficient strength at minimal weight cost. The wing structure comprised of ribs made of mainly balsa while basswood ribs were used at junctions of wing parts and adjacent to payload attachment plate. For 3-D printed parts we considered using PET-G, PLA (Polylactic Acid) and Nylon. Nylon was rejected for its flexible nature and under loads marginally changed the orientation of connecting components. Motor mount had the highest induced stresses, for which we selected PLA as it had the highest yield stress. We wanted to reduce the component weights by gradually reducing infill densities and testing strengths. PET-G proved to be able to sustain similar loads with lower component weight, which was attributed to its lower brittleness than PLA, capable to endure greater plastic deformation than the latter.

3.4 Interfaces and Attachments

FUSELAGE

Motor Mounting
3-D printed PLA firewall is used to attach the motor to the airframe.

Avionics Bay
Avionics attached to the tail boom using Velcro straps as a substitute for the fuselage.

Wing Mounting
3D printed PET-G wing mount is used to connect the wing to the airframe.

WING

Wing Attachment
Pipes are attached to plywood plates through slots using zipties.

- ELECTRONIC
- MECHANICAL
- MAGNETIC

Pipe Attachment
Pipes are attached to plywood plates through slots using zipties.

EMPENNAGE

Boom Locking
Elastic pin with protrusion allows sliding of tubes over each other.

Boom Locking
Pin decompresses on hole alignment and locks the tubes.

Tail Locking
3-D printed PET-G connector fixes empennage to tail boom.

4.0   Loads, Environments and Assumptions

4.1   Designed Load Derivation
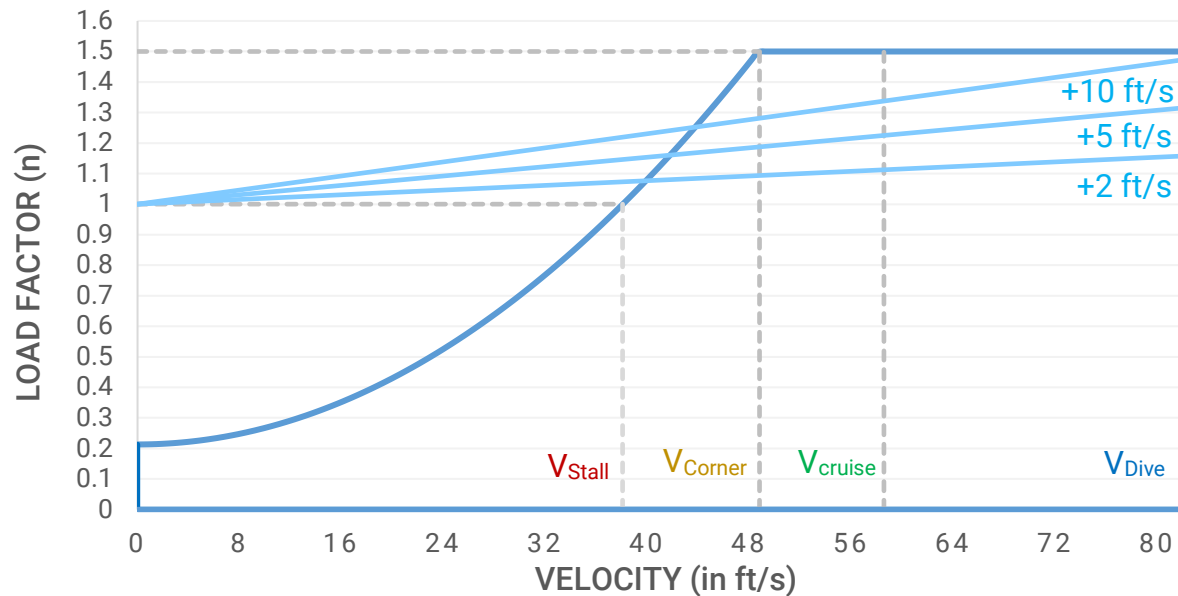
1.   V-n Diagram

Figure 4(a): V-n Diagram

Figure 4(a) depicts the V-n diagram for our aircraft. A non-zero load factor is produced when the aircraft is stationary as lift is generated at the wing due to the effect of prop wash. The maximum load factor has been defined by the integrity of the airframe. Only positive load factors have been considered as the airplane is not designed to fly inverted.

2.   Landing Shock

We derived the impact loading on the airframe during touchdown by calculating change in momentum and normal force. We used accelerometer data to accurately predict the former and assumed approach velocity to be equivalent to stall speed. The median impact time was recorded as 0.2 seconds from multiple flight tests. Glideslopes of 3º, 5º and 10º were considered.

Glideslope (°)	Sink Rate (ft/s)	Impact Loading (lbf)
3	2.74	0.617
5	4.57	1.028
10	9.11	2.049

Table 4(b): Landing Shock Calculation

4.2   Environmental Consideration

Mumbai is subjected to calmer weather. Based on previous experiences, we noted the gusty wind conditions of the competition site and tested our aircrafts at similar locations in India. This was done to ensure the aircraft's performance in competition. The air density change was also accounted, with Mumbai having 0.0728 lb./ft³ during the testing phase and Lakeland having 0.0755 lb./ft³ during the competition. We predicted a 4% increase in the performance of the design.

5.0   Analyses

5.1   Analysis Techniques

5.1.1 Analytical Tools

We used various analytical tools to design and optimize our aircraft to obtain the desired performance.

1. Solidworks

Flow simulation was used to compare design iterations for highest system efficiency, along with using techniques of dynamic meshing and inflation to compare boundary layer separation and effectiveness of drag reduction devices.

Topology optimization techniques were used to achieve the highest overall strength to weight ratio, and provide insight into system level structural inadequacies.

It was also used for accurately predicting the center of gravity and for mass balancing.

2. XFLR5

XFLR5 was used to obtain airfoil polars. It is also used for the stability analysis of the system, to determine longitudinal and lateral dynamic stability eigenvalues.

3. MATLAB & Microsoft Excel

Used for analyses and optimization of system variables using advanced techniques of surrogate modelling and genetic optimization to reach the desired efficiency. They were used to formulate and plot optimum strategies for scoring, launch performance and flight stability.

5.1.2 Developed Models

To predict the trajectory of the aircraft after launch, we developed differential equations for vertical and horizontal displacement with respect to time. We expressed the dynamic thrust, lift and drag as functions of velocity and solved for time, as elaborated in Appendix A.

For turning flight, we analyzed the free body diagram of our aircraft while banking. Horizontal and vertical components of lift were equated to centrifugal force and weight respectively. After simultaneously solving these equations, we obtained the maximum angle of bank and minimum turning radius.

We also developed a model for dynamic thrust, which utilizes propeller air ejection velocity and static thrust values to estimate thrust at various velocities.

5.2   Performance and Sensitivity Analysis

5.2.1 Dynamic Thrust

We analyzed the dynamic thrust characteristics of various motor propeller combinations, as described in **Section (6.0)**. Figure 5(a) compares three of the best combinations.

5.2.2　Launch Performance

Using the developed model as mentioned in Section 5.1.2, we predicted the aircraft trajectory after launch for varying payload fractions, in different weather conditions. Deviations increase with time, as the angle of attack remains constant only for a short time after launch.
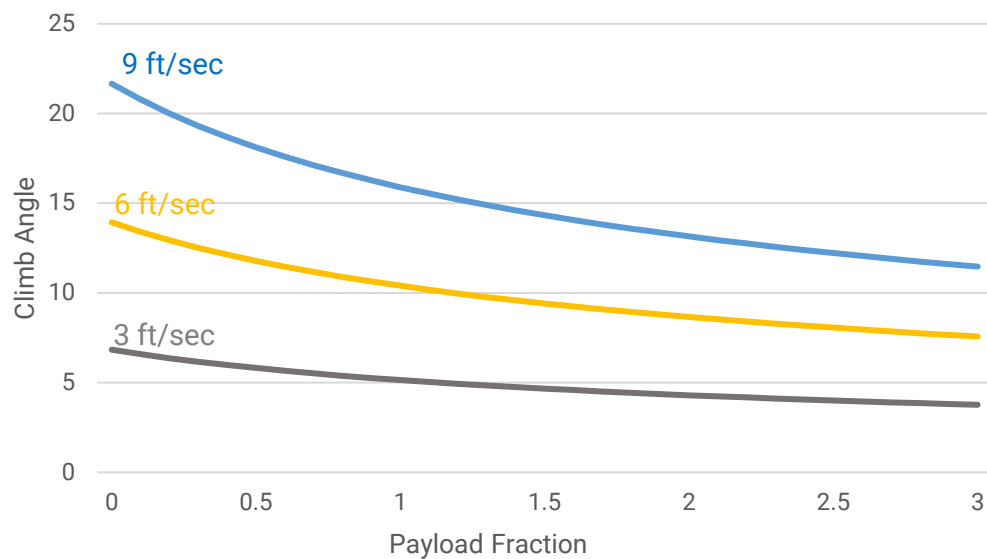
Figure 5(a): Take-off and climb-out performance

5.2.3 Flight and Maneuver Performance

According to the model developed for turning flight, as elaborated in Section 5.1.2 we calculated the maximum angles of bank and minimum turning radii for varying payload weights. The corresponding values have been tabulated in the figure below.
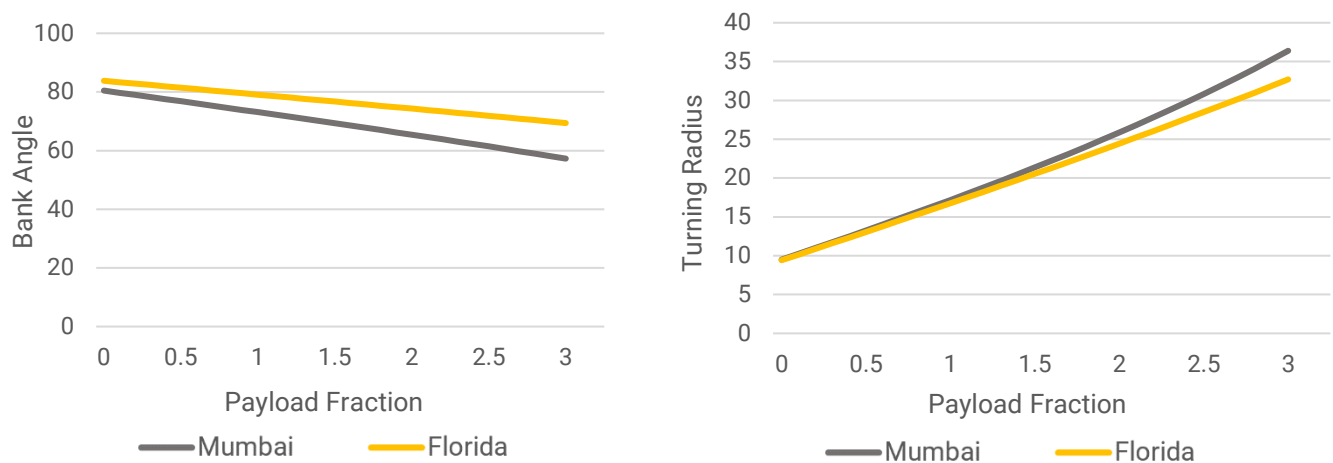
Figure 5(b): Manoeuvre Performance

5.2.4 Static and Dynamic Stability

The negative slope of the C_M vs α curve in Figure 3(i) indicates that the aircraft is statically stable. The neutral point is 7.5" from the aircraft datum and the static margin is 24% of mean aerodynamic chord. Dynamic stability of the aircraft was analyzed using Stability Analysis in the XFLR5. Listed below are the Lateral Stability Eigenvalues for the aircraft
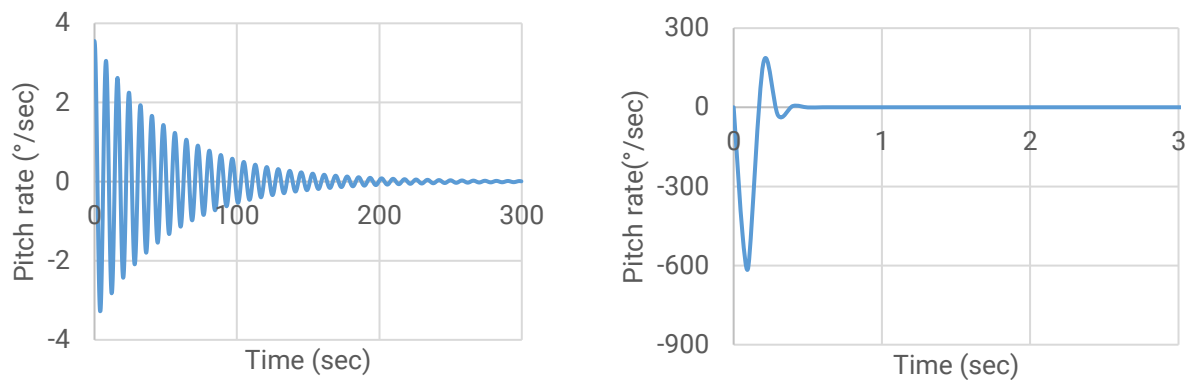

Figure 5(c): Time response for phugoid and short period motion

Roll Dampening	-411.962	Dutch Roll	-5.63±3.904	Spiral Instability	2.200

Table 5(d): Lateral Stability Eigenvalues

Longitudinal Stability: The above graphs depict the time response of the aircraft about the lateral axis in pitch rate (degrees/second) versus time (seconds). The damping factors and times of oscillation being 0.585 and 1.4456 seconds for Short-period mode, and 0.043 and 2.9411 seconds for Phugoid mode respectively. The values were calculated by formulae from [1] using Longitudinal Stability Eigenvalues obtained from XFLR5. Due to the small size and mass of the aircraft, it has greater sensitivity to turbulence, thus a gyro was used to aid in the longitudinal and lateral stability.

5.2.5 Drag Polar Analysis

We analyzed the drag contribution of each sub-assembly of the aircraft, as represented below in the form of a pie chart. The table indicates different values of induced and total drag at various angles of attack
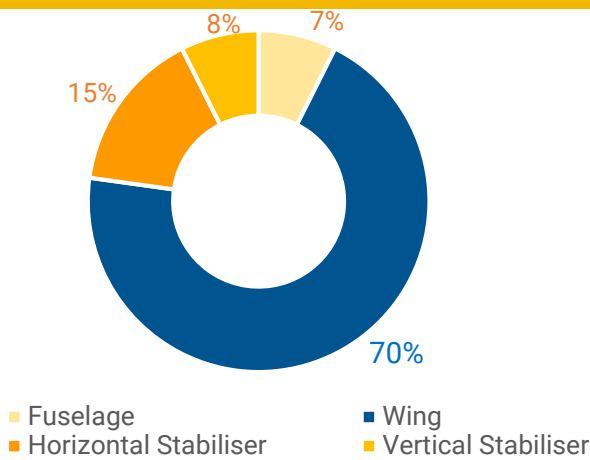
Figure 5(e): Drag Distribution

α	CDo	Cdi	CD
0˚	0.010	0.062	0.072
2˚	0.010	0.080	0.091
4˚	0.010	0.101	0.112
6˚	0.010	0.124	0.135
8˚	0.010	0.149	0.159
10˚	0.010	0.175	0.185

Table 5(f): C_D at Varying Angle of Attack

5.3 Structural Analyses

5.3.1 Applied Loads and Critical Margins

1.   Primary Spar Analysis
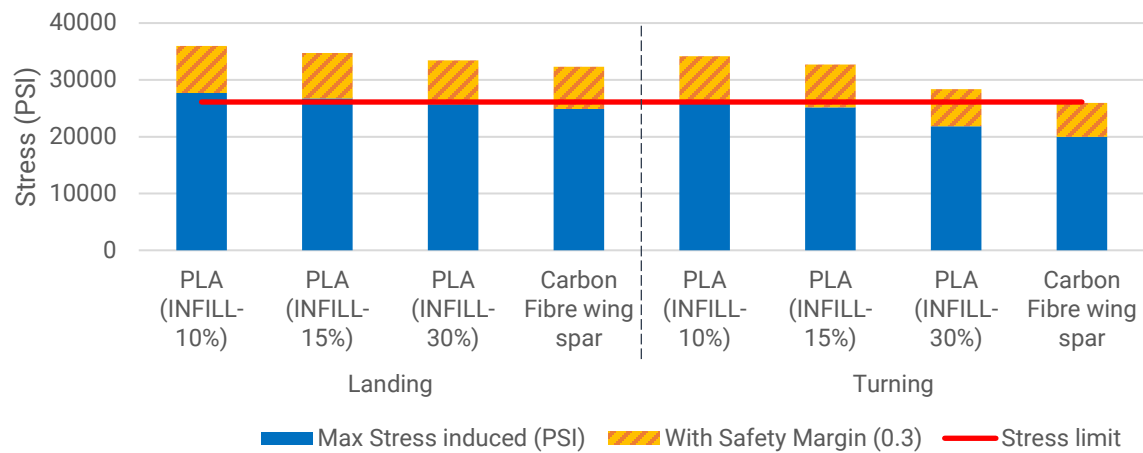
Figure 5(g): Primary Spar Analysis

We tested material alternatives for primary spars which included 3D printed PET-G structures of varying densities and infill percentages. UTM testing was performed to identify material properties which indicated that PET-G cannot sustain loads in corner cases.

2.   Critical Margins

Material	Location	Max Stress induced (PSI)	Max Allowed Stress (PSI)	FOS
Balsa	Wing Airfoils	1090.764544	1914.498138	1.595702536
Basswood	Wing Junctions	1199.783854	2552.664184	2.340252256
Carbon Fibre	Tail Boom	2952.098114	18606.89137	6.302937997
PET-G	Tail Attachment Block	6455.094628	8731.271811	1.352617167

Table 5(h): Critical Margins

5.3.2 Mass Properties and Balance
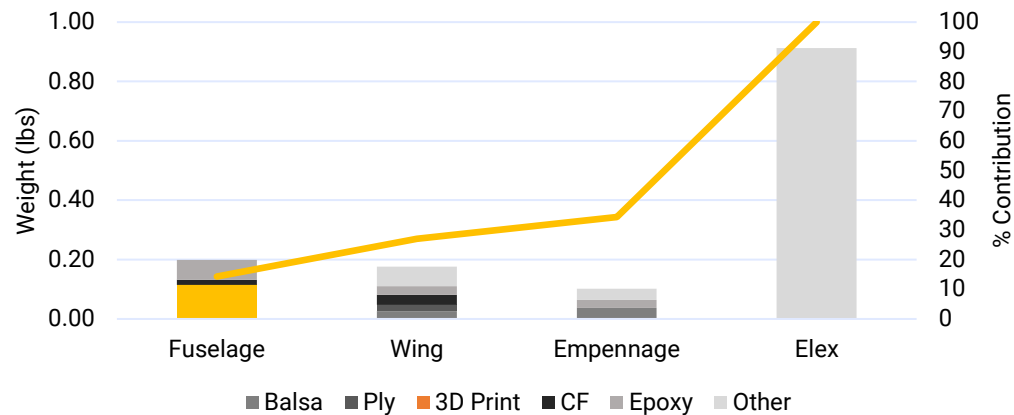
Figure 5(i): Weight Build-up

6.0 Subassembly Testing and Integration

1. Propulsion System
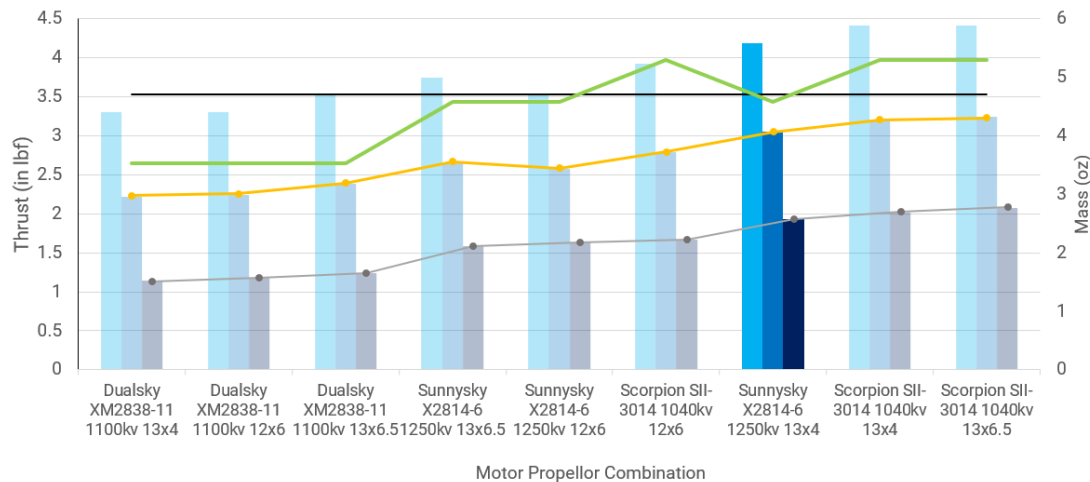
Figure 6(a): Thrust Comparison

Motors were shortlisted after comparing data of static thrust on an online calculator, eCalc,

keeping in mind the practicality of weights for scoring. The dynamic thrust performance was

evaluated using the values sourced from APC propeller performance data sheets, after which

the options were further narrowed down.

We recognized the importance of static and dynamic thrust and performed empirical testing to

identify sensitive parameters, including air ejection velocity and RPM (Rotations per minute).

We tested the dynamic thrust using a wind tunnel. To measure thrust we used a load cell

mounted vertical on a pedestal. The motor mount was attached to the free end of the load cell and the data was calibrated and logged using Arduino UNO. All propellers are APC propellers.

2. Servo testing

The torque produced at the hinge depends on servo arm and control surface sizing, so we constructed an apparatus to measure the torque available at the hinge for their different lengths.

3. Battery Testing

Battery endurance was tested by operating the motor statically at full throttle for the time taken to complete 2 circuits. Once it endured the static test, we cross verified the battery usage during flight test for the same scenario. 850mAh battery although gave just enough flight time, the performance output deteriorated through flight time by up to 20%. We opted to use 1050mAh battery instead.

4. CG Testing and Verification

Aircraft stability is highly sensitive to the position of CG with the respect to the neutral point. The manufactured model was tested for verification of the CG position with its designed position. Its effect after loading on the necessary tail force in dynamic conditions was also analyzed and verified. We used pilot inputs as a feedback for fine-tuning the tail deflection.

5. Flight testing

We conducted flight tests to analyze aircraft performance in real world scenarios. Sensors including RPM sensor, GPS (Global Positioning Sensor) sensor, accelerometer, Pitot tube, and altimeter were incorporated in the telemetry. Flight rounds were conducted with an incremental weight buildup strategy, with the maximum lifting capacity judged from pilot

feedback. We used the data gathered at flight tests to design the aircraft towards having higher lifting capacities.

7.0 Manufacturing

The ribs of wings and tail plates were laser cut on balsa and basswood. Wing was assembled using true scale view of design and aligning components with it. We used cyanoacrylates to hold the structure in place. The design requires precise small cuts which were made using electric tools for stability and jigs for alignment. The 3-D printed parts were layered with a mixture of epoxy and ethyl alcohol solution in 1:10 ratio. Two-part resin-based epoxy was used at critical loading points which include payload carrying plate in wings and attachment of 3-D printed components to respective sub-assemblies. Aerodynamic assemblies of wing and tails were covered with thin covering film to maintain outer mold line.

8.0 Conclusion

As per the report above, we have designed an aircraft which is capable of carrying 50" long payload. We have used unique combinations of materials to ensure structural soundness, as well as performed extensive empirical testing to back our calculations. We hope to make the most of the opportunity the competition provides us, and be competitive against teams from around the world at SAE Aero Design East 2020.

References:

1. Anderson, John D., "Introduction to Flight: Its Engineering and History.

2. Caughey, David A., "Introduction to Aircraft Stability and Control Course Notes"

3. Nicolai, Leland M. and Grant Carichner., "Aircraft Design"

4. Sadraey, Mohammad H., "Aircraft Design: A Systems Engineering Approach"

5. Team 029, DJS Skylark Regular Class Design Report, SAE Aero Design West 2019

Appendix A – Backup Calculations

Servo Calculations:

$$\text{Servo Torque Required} = (8.5 \times 10^{-6}) \frac{c^2 \times v^2 \times \text{control surface span} \times \sin^2(S_1)}{\cos(S_1) \times \tan(S_2)} \times \frac{\text{control horn height}}{\text{servo arm length}}$$

Gust Induced Load factor as a function of gust speed:

$$n = 1 + \frac{k_g V_{gE} V_E \alpha \rho S}{2mg}$$

Aircraft Corner Speed (V*):

$$v* = \sqrt{\frac{2n_{max}mg}{\rho S C_{L_{max}}}}$$

Turning Radius Calculations: (Section 5.2.3)

$$\emptyset = \cos^{-1}\left(\frac{W}{L}\right), R = \frac{mv^2}{L\sin\emptyset}$$

Trajectory Calculations: (Section 5.1.2)

Velocity during hand launch is taken as 40 ft/s and initial pitching angle and angle of attack is taken as 10˚. Cl at 10˚ angle of attack is 1.61204.

$$\sum F_y = ma_y = T\sin\theta + L\cos\theta - D\sin\theta - mg$$

$$\sum F_x = ma_x = T\cos\theta - L\sin\theta - D\cos\theta$$

$$S_y(t) = \iint a_y \, dt^2$$

$$S_x(t) = \iint a_x \, dt^2$$

Thrust Calculations: (SECTION 5.1.2)

$$T = \rho(\pi d^2/4)\,(v^2 - v_e v)\beta = 0.28599 \times (52.493 - v) \times 0.763627$$

Take-off and Landing Analysis: (SECTION 5.1.2)

$$v^2 > \frac{mg}{\frac{1}{2}\rho S C_L} \qquad \dots (1)$$

$$\text{Thrust} - \text{Drag} - \text{Friction} = \text{Mass x Acceleration} = mv\,dv/dx \qquad \dots (2)$$

$$S_{TO} = \int dx = \int \frac{mvdv}{\{T(v)-[D(v)+\mu(W-L(v))]\}}$$

The take-off distance is the value of x obtained after integrating (2), for the velocity obtained

from equation (1).

Damping Factor:

$$\zeta = \frac{1}{\sqrt{1 + (\frac{2\pi}{\delta})^2}} \qquad \text{where} \qquad \delta \triangleq \ln \frac{x_1}{x_2}$$

Where x_1 and x_2 are the vibration amplitudes at two successive peaks of the decaying

vibration and δ is the logarithmic decrement.

Landing Shocks:

Impact = Normal Reaction + Impulse

Impulse= Momentum/Impact time

.

SAE AERODESIGN EAST 2020

APPENDIX B
Technical Data Sheet – Weight Build Up (Micro Class)
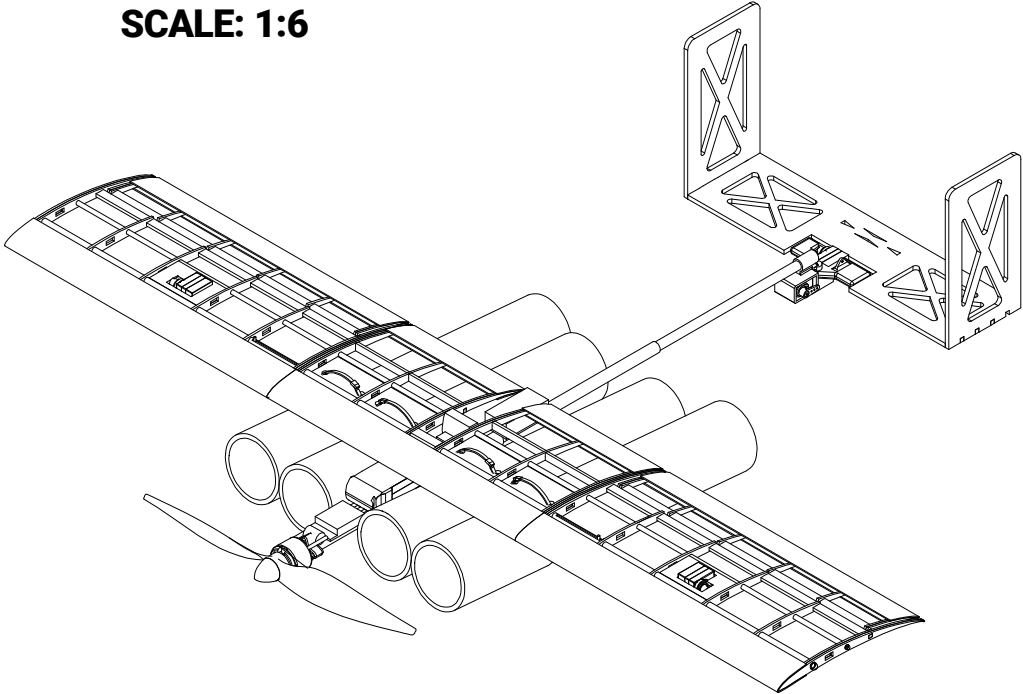
Team Name: DJS Skylark - Micro

Team Number: 312

School Name: Dwarkadas J Sanghvi College Of Engineering

	Components	Weights (lbs)
1	Propeller	0.0705
2	Motor Assembly (Motor, Motor mount, spinner nuts, and bolts)	0.2954
3	Battery	0.2138
4	Receiver	0.0243
5	Electronic Speed Controller	0.0661
6	Aileron Servo (Quantity: 2)	0.0661
7	Horizontal Stabilator Servo	0.0331
8	Rudder Servo	0.0331
9	Red Arming Plug	0.0441
10	Electronic Wire Extensions	0.0661
11	Centre Wing	0.0441
12	Right Wing	0.0661
13	Left Wing	0.0661
14	Wing Mount	0.0661
15	Tail Mount	0.0331
16	Tail Boom	0.0882
17	Horizontal Tail	0.0353
18	Vertical Tail	0.0331
19	Zip Ties	0.0441
		Total:1.3889

AIRCRAFT SUMMARY DATA

WINGSPAN	MAC	TMA	EMPTY WEIGHT	BATTERY	MOTOR MODEL	MOTOR KV	PROPELLER	SERVO (Aileron) (A)	SERVO (ELEVATOR) (B)	SERVO (RUDDER) (C)
34.2 ± 0.1"	6.5"	18.3 ± 0.1"	1.389 lbs	Tattu 1050mAh 3S 75C LiPo	Sunnysky X2814-6 14 Poles	1250KV	APC 13x4E	Turnigy TGY 9018-MG (34.72 oz-in)	Turnigy TGY 9018-MG (34.72 oz-in)	Turnigy TGY 9018-MG (34.72 oz-in)

ISOMETRIC VIEW
SCALE: 1:6

28.1 ±0.1

MAC: 6.5 ±0.1

FORE CG 5.8
LOADED CG 5.8 STATIC MARGIN 13.8%
AFT CG 6.0
EMPTY CG 6.0 STATIC MARGIN 10.8%
NEUTRAL POINT 6.7

SOLIDWORKS Educational Product. For Instructional Use Only.

34.2 ±0.1
11.7 ±0.1
6.3

WEIGHT AND BALANCE TABLE

SR NO.	COMPONENTS	WEIGHT (lbs)	ARM (in)	MOMENT (lbs-in)
1	MOTOR	0.2800	-0.5894	-0.1650
2	BATTERY	0.2100	5.9459	1.2486
3	PAYLOAD	2.5813	5.9460	15.3484
4	ELECTRONICS	0.4189	6.0460	2.5327

BASIC DIMENSIONS

LENGTH	28.1 ± 0.1"
WIDTH	34.2 ± 0.1"
HEIGHT	6.3 ± 0.1"

Team NO: 312
Team Name: DJS Skylark - Micro Class

School Name: Dwarkadas J. Sanghvi College of Engineering

SAE Aero Design East 2020

Size: B   Scale: 1:8   Unit: inches

Page: 27